Chapter 4

Biological Particle Control and Separation using Active Forces in Microfluidic Environments

Mohd Anuar Md Ali,
Aminuddin Bin Ahmad Kayani and
Burhanuddin Yeop Majlis

Additional information is available at the end of the chapter

http://dx.doi.org/10.5772/intechopen.75714

Abstract

Exploration of active manipulation of bioparticles has been impacted by the development of micro-/nanofluidic technologies, enabling evident observation of particle responses by means of applied tunable external force field, namely, dielectrophoresis (DEP), magnetophoresis (MAG), acoustophoresis (ACT), thermophoresis (THM), and optical tweezing or trapping (OPT). In this chapter, each mechanism is presented in brief yet concise, for broad range of readers, as strong foundation for amateur as well as brainstorming source for experts. The discussion covers the fundamental mechanism that underlying the phenomenon, presenting the theoretical and schematic description; how the response being tuned; and utmost practical, the understanding by specific implementation into bioparticles manipulation engaging from micron-sized material down to molecular level particles.

Keywords: microfluidics, nanofluidics, dielectrophoresis, magnetophoresis, acoustophoresis, thermophoresis, optical tweezing, optical trapping

1. Introduction

Progress in biomedical technologies has emerged into miniaturization of biomedical devices. The main features in miniaturized biomedical devices are establishment of controlled microenvironment that promotes predictive micro-/nanoparticle behaviors and reduction in required sample volume for characterization of scarce materials, e.g., patient-derived samples, which help to reduce the cost and time for diagnosis and therapy [1]. Miniaturization of these biomedical devices demands for implementation of particular procedures in precise approach, which has

been extensively studied in micro-/nanofluidic system integrated with active manipulation mechanisms [2–4].

Micro-/nanofluidic system facilitates researchers in creating well-controlled micro-/nanoscale environment and at the same time enables the analysis of micro-/nanoparticles including biological particle (bioparticle) behaviors and responses toward active manipulation mechanisms, in addition to particle-particle reactions and external stimuli [5]. Active manipulation mechanisms make possible the control of bioparticle displacement and motional trajectories in a highly predictable and consistent fashion [2], by introducing tunable external force systems such as dielectrophoresis (DEP) [6, 7], magnetophoresis (MAG) [8], acoustophoresis (ACT) [9], thermophoresis (THM) [10], and/or optical tweezing/trapping (OPT) [11, 12].

In this chapter, description of the fundamental mechanism underlying the phenomenon is presented, covering the theoretical and schematic description, as well as specific implementation into bioparticle manipulation covering from micron-sized material down to molecular-level particles. Conclusion and future perspectives of this multidisciplinary field are provided at the end of this chapter.

2. Bioparticles in biomedical studies

Manipulation of bioparticles has been a major concern in recent development of micro−/nanofluidic studies due to their potential in biomedical application. Those particles, according to their biological structure and physical properties, can be categorized as (1) model organisms; (2) body cells, which include blood cells, tumor and cancer cells, and stem or progenitor cells; (3) bacteria; (4) viruses; (5) nucleic acids; and (6) proteins.

Model organisms, either unicellular (e.g., yeast) or multicellular (e.g., *Danio rerio* zebrafish, *Caenorhabditis elegans* nematode, etc.), are being used for cellular process studies (cell cycle, cell division, metabolism, etc.), genetic and pharmacological studies, as well as pathogenesis and therapy studies. Blood which composed by two components, i.e., (1) blood plasma and (2) the formed elements, including red blood cells (RBCs), white blood cells (WBCs), and platelets, is of high interest as they are being used in various health check and clinical tests, such as blood test to determine whether our organs (e.g., kidneys, liver, thyroid, heart, etc.) are working properly and to diagnose any disease such as HIV/AIDS, cancer, anemia, diabetes, and coronary heart disease. Tumor cells (benign) and cancer cells (malignant) are cells that undergo uncontrolled proliferation, causing tumor development either at the skin, colon, rectum, prostate, breasts, or lungs. They are grouped either as (1) carcinomas (develop in epithelial cells), (2) leukemia and lymphomas (develop at the blood and lymphatic system), or (3) sarcomas (develop at the connective tissue). These cells attempt to develop secondary tumor (metastasis tumor) by spreading through vascular or blood vessel network in the form of circulating tumor cells (CTCs). Stem cells, either adult stem cells or pluripotent stem cells, are cells that can self-renew, generating perfect copies of themselves by division and differentiation, where the produced cells are specific for certain function in the body. These cells are important in research, drug screening test, and cell transplantation therapy. Bacteria, which are unicellular

prokaryotic microorganisms, grow and reproduce rapidly through binary fission. They are important in biomedical studies in the development of disease diagnostic tools and in understanding of biological responses under certain stimuli, according to their actions, either as predators, mutualists, or pathogens, in which pathogenic bacteria demonstrate a parasitic association with other organisms to cause infections. Viruses, which are genes enclosed by a protective coat, are infective agents due to lack of metabolic machinery, hence depending on the host for gene expression. They are important in the study of virus detection as well as the study of virus influence to cells. Nucleic acids, which are biomolecules made from nucleotides as monomers, function in encoding, transmitting, and expressing genetic information. There are two types of nucleic acids in living cells, which are deoxyribonucleic acid (DNA) and ribonucleic acid (RNA). They are highly essential in the research of replication, repair, storage and modification of DNA, disease biomarkers, and gene delivery. Proteins are biomolecules constructing a single or a number of long chains of amino acid residues. The discovery of their role within living organisms includes catalyzing metabolic reactions, DNA replication, responding to stimuli and transporting molecules from one location to another, and getting remarkable attention in the biomedical research and application these days.

3. Dielectrophoresis

Dielectrophoresis (DEP) is the motion of polarizable particles under a spatially nonuniform electric field that cause momentary polarization of the particle by dipole establishment within, with an unequal Columbic forces at both ends of the particles, causing the particles to move [2, 6, 7].

3.1. Fundamentals of DEP

Dielectrophoretic force, F_{DEP}, for a stationary alternative current (AC) field is given by

$$F_{DEP} = 2\pi a^3 \varepsilon_m \mathrm{Re}[f_{CM}] \nabla |E|^2 \tag{1}$$

where E is the electric field, ε_m is the permittivity of the suspending medium, a is the particle radius, f_{CM} is the Clausius-Mossotti factor which describes relationship between dielectric constants of two different media, and the Re[f_{CM}] is the real part of the factor [7].

For a spherical particle, f_{CM} is governed by

$$f_{CM} = \frac{\varepsilon_p^* - \varepsilon_m^*}{\varepsilon_p^* + 2\varepsilon_m^*} \tag{2}$$

where ε^* is the complex permittivity, which is determined by

$$\varepsilon_{p,m}^* = \varepsilon_0 \varepsilon_{p,m} - j\frac{\sigma_{p,m}}{\omega} \tag{3}$$

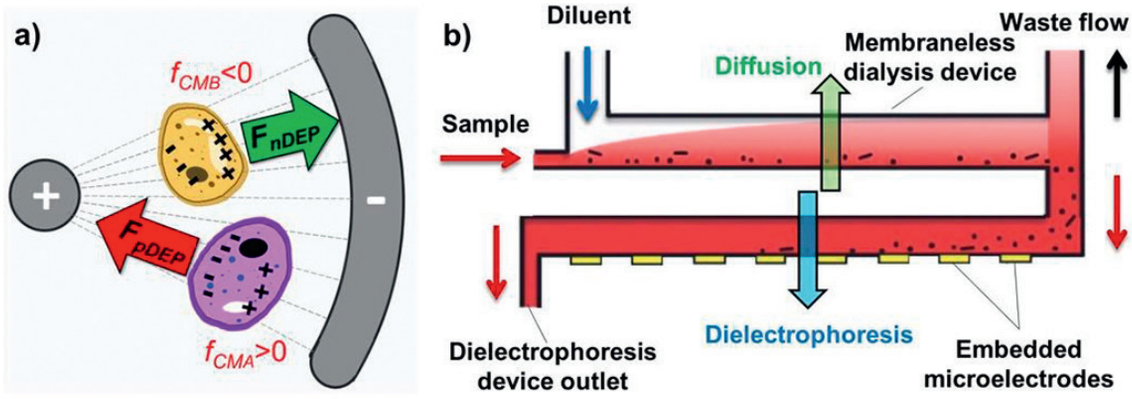

Figure 1. (a) Dielectrophoresis. At a certain frequency, particle A (purple) experiences higher polarizability than the suspending medium ($f_{CMA} > 0$), attracting it to the region with higher electric field gradient, while at the same time particle B (yellow) experiences less polarizability than the suspending medium ($f_{CMB} < 0$), pushing it away to the region with lower electric field gradient (F_{pDEP}, positive dielectrophoretic force; F_{nDEP}, negative dielectrophoretic force) (Reprinted with permission from Md Ali et al. [13]. Copyright 2016 Royal Society of Chemistry). (b) Manipulation of bacteria by dielectrophoresis. Blood specimen mixed with a permeabilizing agent sample is injected into the microfluidic device for desalination process by membraneless dialysis before subsequent enrichment of target bacteria, *E. coli*, at dielectrophoretic electrodes (Adapted with permission from D'Amico et al. [14]. Copyright 2017 Royal Society of Chemistry).

where ε_0 is the vacuum permittivity (8.854×10^{-12} F/m, j is the unit imaginary number, i.e., $\sqrt{(-1)}$, σ is the conductivity, and ω is the angular frequency of electric signal supplied. The subscripts "p" and "m" stand for the particle and the medium, respectively.

The dielectrophoretic force direction is determined by the sign of the f_{CM}, as presented in **Figure 1a**. For f_{CM} with positive sign ($f_{CM} > 0$), the force pulls particles to the region with high electric field gradients, and the situation is termed as positive DEP (pDEP). While for f_{CM} with negative sign ($f_{CM} < 0$), the force pushes particles away from those regions, and this is termed as negative DEP (nDEP). Hence, the dielectrophoretic force is proportional to particle volume and is highly dependent on the electrical properties of the particle, the medium, and the frequency of the AC field [15].

Moreover, for an AC field with spatial variation, the dielectrophoretic force is given by

$$F_{DEP} = 2\pi\varepsilon_m \mathrm{Re}[f_{CM}]\, a^3 \nabla |E|^2 + 2\pi\varepsilon_m \mathrm{Im}[f_{CM}]\, a^3 \times \left(|E_i|^2 \nabla \varphi_i\right) \quad (4)$$

where Re[f_{CM}] and Im[f_{CM}] are the Clausius-Mossotti real part and imaginary part, respectively; φ is the AC field phase, and subscript "i" represents each element of the field as well as the phase [15]. AC field with spatial variation is being employed in (1) traveling wave DEP and (2) electrorotation.

In general, the traveling wave DEP is created by application of 90° phase-shifted electric signal, i.e., 0, 90, 180, and 270°, on an array of planar parallel electrodes, causing generation of a traveling wave of electrostatic potential which can vertically suspend a lossy dielectric sphere while at the same time propels it along the array. The Re[f_{CM}] determines whether the bioparticles are levitated (nDEP) or attracted to the electrodes (pDEP), while Im[f_{CM}] determines the

http://dx.doi.org/10.5772/intechopen.75714

translational movement in direction of electrode array. The electrorotation employs quadrupole electrodes with 90° phase-shifted electric signal. The electrodes generate a rotating electric field when excited with this multiphase AC field. Electrorotation is achieved by nDEP ($\mathrm{Re}[f_{CM}] < 0$) for bioparticle levitation during the rotational motion which is determined by $\mathrm{Im}[f_{CM}]$ [16].

As bioparticles are typically multilayered with the presence of multilayer membranes, Clausius-Mossotti factor calculation needs to consider total permittivity of the bioparticle comprising of the permittivity of all layers. Total permittivity, ε_p, for a spherical multilayered particle is given by

$$\varepsilon_p = \varepsilon_{p_n}\left[\left(\frac{a_n}{a_{n-1}}\right)^3 + 2\left(\frac{\varepsilon_{p_{n-1}} - \varepsilon_{p_n}}{\varepsilon_{p_{n-1}} + 2\,\varepsilon_{p_n}}\right)\right] \Bigg/ \left[\left(\frac{a_n}{a_{n-1}}\right)^3 - \left(\frac{\varepsilon_{p_{n-1}} - \varepsilon_{p_n}}{\varepsilon_{p_{n-1}} + 2\,\varepsilon_{p_n}}\right)\right] \tag{5}$$

where ε_{p_n} is the permittivity that includes the outermost layer of the bioparticle, while $\varepsilon_{p_{n-1}}$ is permittivity that excludes the outermost layer. a_n is the outermost layer (e.g., cell wall) radius, and a_{n-1} is the second outermost layer (e.g., membrane) radius. The denotation $n = 0, 1, 2, 3\ldots$ is the corresponding layer calculation number that starts from the innermost layer ($n = 0$). The total permittivity, ε_p, is the final layer calculated permittivity, ε_{p_n}, in which n is the final layer number [16].

Transition between the pDEP and nDEP responses of bioparticle happens across the point when the polarization of the particle and the suspending medium are equal, which occurs at a particular frequency known as crossover frequency, f_{xo}. For a spherical structure, f_{xo} is governed by

$$f_{xo} = \frac{\sqrt{2}\,\sigma_m}{2\pi a\, C_m} \tag{6}$$

where σ_m is the conductivity of the surrounding medium, a is the particle radius, and C_m is the capacitance of the bioparticle plasma membrane [17].

3.2. Dielectrophoretic manipulation of bioparticles

Manipulation of model organism has been demonstrated by Chen et al. [18], who perform detection and trapping of *Shewanella oneidensis*, a model organism for electrochemical activity bacteria, using DEP microfluidic chip, which equipped with real-time imaging for trapping process observation. The trapping is enhanced by providing hole arrays on top of the electrode, in which the hole size-bacteria count relation is also studied. Sang et al. [19] demonstrate blood manipulation using DEP. A portable microsystem for separation of living/dead RBCs by DEP which integrated with subsequent evaluation using surface stress sensor for living/dead RBC detection has been developed. This multifunctional portable microsystem is of potential application into diagnostic of hemolytic anemia disease, i.e., the situation where RBCs are damaged and removed from the bloodstream before their normal lifespan is over. Chiu et al. [20] use optically induced DEP (ODEP) to enhance conventional microfluidic isolation and purification of CTCs from whole blood sample. In this system, light image is projected on photoconductive materials which coated on indium tin oxide (ITO) glass substrate to generate dielectrophoretic force field. Hollow circular images are used for targeted CTC

trapping, while long rectangular light bar is used to attract other untargeted cells. Adams et al. [21] perform sorting of neural stem and progenitor cells using microfluidic DEP device. The sorting is based on the cell membrane capacitance variation, which specifically determines the future forming cells, either neuron or astrocyte. Bacteria manipulation using DEP microfluidic device is shown by D'Amico et al. [14], in which they isolate and enrich *Escherichia coli* (*E. coli*) which spiked into whole blood sample. The device integrates membraneless dialysis process and dielectrophoretic trapping, presented in **Figure 1b**. Ding et al. [22] demonstrate the capture and enrich of *Sindbis* virus in a gradient insulator-based DEP microfluidic device, i.e., electric signal source is applied across both microchannel ends while insulating polydimethylsiloxane (PDMS) used to distort electric field, hence forming a nonuniform electric field. By tuning the voltage of applied signal, they can capture or release the virus from the saw-shaped electrode tip. Nucleic acid manipulation has been conducted by Jones et al. [23], in which they perform size-based sorting of a wide range of nucleic acid analytes, i.e., 1.0, 10.2, 19.5, and 48.5 kbp double-stranded DNA (dsDNA) analytes, including both plasmid and genomic DNA in a continuous flow microfluidic platform, by using an insulator-based DEP to tune the deflection of the nucleic acids. Viefhues et al. [24] perform dielectrophoretic mobility shift assay of DNA complexes as well as pure DNA in a nanofluidic DEP system to demonstrate new technique in detection of different DNA variants, including protein-DNA complexes. Manipulation of proteins has been achieved by Mohamad et al. [25]. They use DEP to capture and characterize the electrical properties of colloidal protein molecule, i.e., bovine serum albumin (BSA), based on the molecule dispersion impedance exhibited at particular frequencies, which are influenced by the electrical double layer surrounding the molecule. Liao et al. [26] developed a DEP nanofluidic device to perform selective pre-concentration of functional proteins within bio-fluid medium, which in general is a high ionic strength medium. The device is advantageous in the enhancement of DEP trapping forces against electrothermal flow which is challenging in nanoscale device design.

4. Magnetophoresis

Magnetophoresis (MAG) is the motion of particles under the influence of a nonuniform magnetic field, as the particles being magnetized cause them to be attracted toward the regions of high magnetic flux density or repelled away [8]. Magnetic field is generated by either a permanent magnet or an electromagnetic coil.

4.1. Fundamentals of MAG

Magnetophoretic force experienced by a particle is governed by

$$F_{MAG} = \frac{(\chi_p - \chi_m) V_p}{\mu_0} (B \cdot \nabla) B \tag{7}$$

where F_{MAG} is the effective magnetic force upon the particle; χ_p and χ_m are the magnetic susceptibility of the particle and the medium, respectively; V_p is the particle volume, B is the magnetic flux density, and μ_0 is the free space permeability [8].

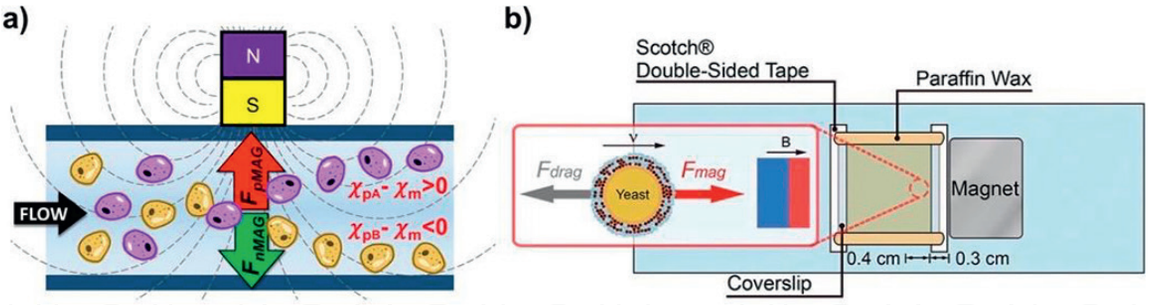

Figure 2. (a) Magnetophoresis. Bioparticles A (purple) are pushed toward the region with maximum magnetic flux density (pMAG) due to positive magnetic susceptibility difference between the bioparticles and the suspending medium (χ_{pA}-χ_m > 0), while bioparticles B (yellow) experience the opposite (χ_{pB}-χ_m < 0), thus being repelled away from the region (F_{pMAG}, positive magnetophoretic force; F_{nMAG}, negative magnetophoretic force) (Reprinted with permission from Md Ali et al. [13]. Copyright 2016 Royal Society of Chemistry). (b) Manipulation of model organism by magnetophoresis. Multilayered magnetic silica film-coated yeast is manipulated in microfluidic device equipped with external permanent magnet (Reprinted with permission from Lee et al. [27]. Copyright 2016 Springer Nature).

The motional direction is controlled by the difference of magnetic susceptibility between the particle and the medium, i.e., χ_p-χ_m. For a positive magnetic susceptibility difference (χ_p-χ_m > 0), the suspended particles are pushed to region with maximum magnetic field flux gradient, and this situation is known as positive MAG (pMAG). In contrast, under negative magnetic susceptibility difference (χ_p-χ_m < 0) situation, the particles are pushed to regions with minimum magnetic field flux gradient, and this is called as negative MAG (nMAG). The conceptual mechanism is shown in **Figure 2a**.

Common practices in magnetophoretic manipulation of bioparticle employ either (1) immunomagnetic manipulation [28] or (2) diamagnetic manipulation [29], in which paramagnetic bounded to bioparticle is exploited in the former, while in the latter, paramagnetic- or ferrofluid-suspending medium is utilized. In immunomagnetic bioparticle manipulation, paramagnetic micro-/nanoparticles, e.g., iron oxide microparticles and streptavidin paramagnetic particles, which have higher susceptibility compared to suspending medium are used. Target bioparticles are bounded to paramagnetic micro-/nanoparticles through antibodies, benefiting from binding affinity with bioparticles. Under influence of magnetic field, the microparticle-bioparticle complexes can be manipulated. While in diamagnetic bioparticle manipulation, a suspending medium with higher magnetic susceptibility compared to target bioparticle is utilized. In this method, the magnetic field manipulates the suspending medium rather than the bioparticles themselves.

4.2. Magnetophoretic manipulation of bioparticles

Lee et al. [27] magnetically functionalize living yeast cells, *Saccharomyces cerevisiae* (*S. cerevisiae*), as micro-magnets, by performing coating of several groups of them with different thicknesses of magnetic silica film (single layer up to seven layers), to control the magnetization degree of the cells as shown in **Figure 2b**. By doing so, multiple subgroups are being formed which can be manipulated independently in the pool of heterogeneous cell mixtures. Magnetophoretic separation of erythrocytes, i.e., maturing RBCs from the mixture with reticulocytes and immature RBCs, in hematopoietic stem cell (HSC) culture, has been performed by Jin

et al. [30]. They exploit the paramagnetic property of deoxygenated hemoglobin of maturing erythrocytes compared to reticulocyte which is diamagnetic for the MAG-based separation. Jack et al. [31] demonstrate immunomagnetic isolation of diverse groups of magnetic bead-labeled tumor cells (with different levels of labeling), based on the surface protein expressions. The sample is introduced to multiple levels of magnetic sorter according to the adjustment of external permanent magnet distance to flowing magnetic-labeled cells, resulting in separation of the cells according to their epithelial cell adhesion molecule (EpCAM) levels into low, moderate, and high expression. Bacteria manipulation using MAG has been achieved by Wang et al. [32], who demonstrate the trapping of *Bacillus megaterium*, which are nonmagnetic bioparticles in a ferrofluid suspension while experiencing uniform external magnetic field. The sample continuously flows in a microfluidic channel with nonmagnetic island located in the middle of the channel. Due to the magnetic susceptibility difference between the island and the surrounding ferrofluid, the nonmagnetic bacteria experience magnetophoretic force and, thus attract the bacteria to the island, while the ferrimagnetic particle which comprises the ferrofluid is also attracted to the island; however, the bacteria and the magnetic particles are accumulated at different regions. Wang et al. [33] perform magnetophoretic concentration of avian influenza virus (H5N1) in continuous flow microfluidic system. The H5N1 magnetic nanoparticle complexes are formed using aptamer-biotin-streptavidin binding and injected to three-dimensionally printed magnetophoretic platform which experiences magnetic field from external neodymium magnets, to migrate the complexes from the original sample flow to phosphate-buffered saline carrier flow. Shim et al. [34] demonstrate the magnetophoretic capture of DNA-conjugated magnetic particles in microfluidic device by short-range magnetic field gradient exerted by micro-patterned nickel array on the bottom surface of the separation channel, as well as enhancement with oppositely oriented array of external permanent magnet for a long-range magnetic field gradient at the interfaces between magnets. The DNA is then collected by performing detachment from the captured DNA magnetic particle conjugates by enzymatic reaction with uracil-specific excision reagent enzyme. Magnetophoretic manipulation of protein has been achieved by Lim et al. [35] in which manipulation of Atto-520 biotin-streptavidin-magnetic particle conjugates is demonstrated. The magnetic force is applied by external rotating magnetic field, while soft permalloy ($Ni_{80}Fe_{20}$) magnetic tracks composed of radii and spiral tracks, known as spider web network, are patterned underneath the manipulation plane. The structure facilitates the directional transportation of magnetic particles, which is of potential application as biomolecule cargo, to the desired path, either converging to the spider web center or dispersing away, according to the external rotating magnetic field, i.e., clockwise or counterclockwise.

5. Acoustophoresis

Acoustophoresis (ACT) is the motion of particles when experiencing a surface acoustic wave (SAW) radiation pressure, either by standing surface acoustic wave or traveling surface acoustic wave [36, 37].

http://dx.doi.org/10.5772/intechopen.75714

5.1. Fundamentals of ACT

Acoustophoretic force, F_{ACT}, experienced by a particle is determined by.

$$F_{ACT} = 4\pi a^3 E_{ACT} k \sin(2kx)\phi \tag{8}$$

where F_{ACT} is the acoustic radiation force, E_{ACT} is the acoustic energy density, a is the particle radius, x is the distance from pressure antinode in the wave propagation axis, k is the wave number ($2\pi f l c_0$), and ϕ is the acoustic contrast factor [9].

The direction of the particle motion, either toward the pressure node or the antinode, is governed by the sign of the acoustic contrast factor, ϕ, given by

$$\phi = \frac{\rho_p + \frac{2}{3}(\rho_p - \rho_m)}{2\rho_p + \rho_m} - \frac{1}{3}\frac{\rho_m c_m^2}{\rho_p c_p^2} \tag{9}$$

where ρ_p and ρ_m are the density of the particle and medium, respectively, while c_p and c_0 are the speed of sound within the particle and medium, respectively. As shown in **Figure 3a**, for a condition with positive acoustic contrast factor (ϕ>0), the particles are pushed toward the pressure node, and the phenomenon is known as positive ACT (pACT). In contrast, for a negative acoustic contrast factor condition (ϕ<0), the particles are pushed toward the pressure antinode, and it is called as negative ACT (nACT).

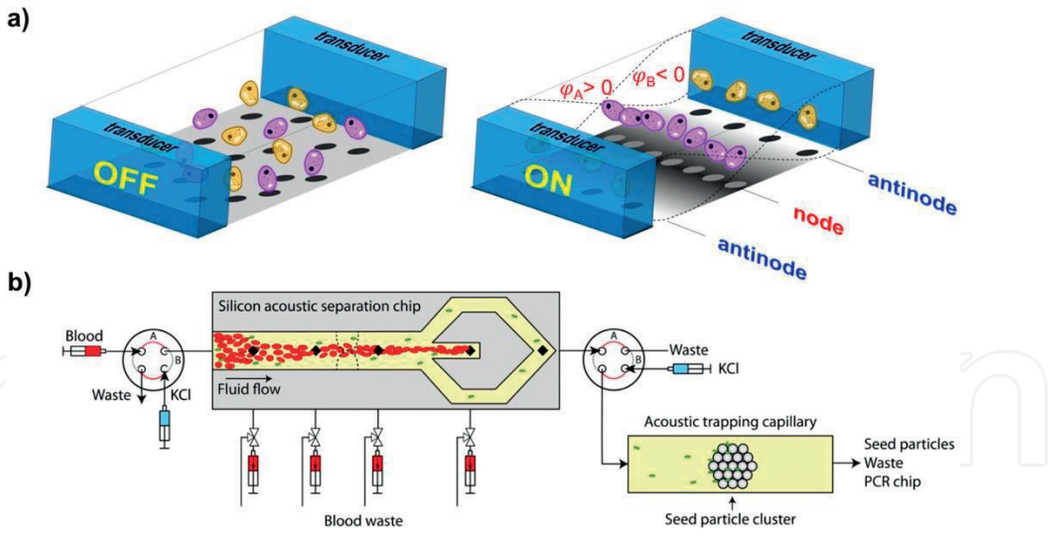

Figure 3. (a) Acoustophoresis. (Left) Bioparticles are randomly dispersed in the suspending medium without the presence of acoustic radiation pressure. (Right) Bioparticles experience acoustic radiation pressure when SAW transducer is turned on. Bioparticles A (purple) are pushed toward the pressure node due to positive acoustic pressure contrast ($\phi_A > 0$). Bioparticles B (yellow) which experience the opposite ($\phi_B < 0$) are pushed toward the pressure antinodes (Reprinted with permission from Md Ali et al. [13]. Copyright 2016 Royal Society of Chemistry). (b) Manipulation of bacteria in blood by acoustophoresis. Separation of bacteria from RBCs is performed by acoustic separation chip. Bacteria enrichment from blood plasma is performed subsequently at acoustic trapping capillary before the release for detection and identification by dry-reagent PCR chips (Reprinted with permission from Ohlsson et al. [38]. Copyright 2016 American Chemical Society).

Mainstream applications of ACT in particle manipulation employ either (1) traveling surface acoustic wave (TSAW) [37] or standing surface acoustic wave (SSAW) [36]. A TSAW is a condition when a surface acoustic wave (SAW) is propagating from interdigitated transducer (IDT) electrodes, while SSAW occurs when two TSAWs constructively interfere and form a standing or stationary SAW. TSAW can be generated by a single IDT electrode, while the SSAW can be generated either by a pair of IDT electrodes or a combination of a single IDT and wave reflectors. In TSAW acoustophoresis, bioparticles move together with the wave propagation, while in SSAW acoustophoresis, they are pushed toward the SAW pressure node or the antinode. Pressure node is the region of constant pressure, while pressure antinodes are regions alternating between maximum and minimum pressure values.

5.2. Acoustophoretic manipulation of bioparticles

Acoustophoretic manipulation of model organism has been demonstrated by Sundvik et al. [39]. They study levitation of zebrafish embryos using acoustic radiation force in a noncontact wall-less platform for a period of less than 2000 s, while the embryos still in development at 2–14 hours postfertilization, and they found that the levitation does not interfere the development, though it might influence mortality rate. Urbansky et al. [40] perform the manipulation of peripheral blood progenitor cells (PBPCs) with the focus on sorting out CD8 lymphocytes (target cells) from the mixture that contains CD4, CD19, CD34, and CD56 lymphocytes as well. They label the CD8 with affinity beads, forming bead-cell complex, to modify the acoustic mobility of the target cells. Furthermore, they modify the medium properties of central buffer, using Ficoll wash buffer, to adjust the acoustic force on different particles, so that bead-CD8 complexes are pushed into central buffer under acoustophoretic force exerted by piezoceramic transducer, while other unbounded cells remain flowing at the side due to lower acoustic mobility. Urbansky et al. [41] further perform separation of mononuclear cells (MNCs) from diluted whole blood using acoustophoretic microfluidic device. They managed to overcome the behavior similarity of MNCs and RBCs in acoustic standing wave by optimizing the buffer conditions to modify the acoustophoretic mobility of the cells. Antfolk et al. [42] accomplish separation of spiked prostate cancer cells (DU145) from whole blood using ACT-DEP-integrated platform consisting of acoustophoretic pre-alignment, separation, and concentration of targeted DU145 cells, prior to single-cell array trapping using DEP microwell. Bacteria manipulation has been accomplished by Ohlsson et al. [38], who developed a microsystem for bacteria separation, enrichment, and detection from blood, as demonstrated in **Figure 3b**. The system is integrated with acoustic separation to remove RBCs from blood sample, with subsequent enrichment of bacteria from plasma by acoustic trapping to polystyrene seed particles, and polymerase chain reaction (PCR) for detection and identification of the bacteria at the final stage. They demonstrate the system using whole blood samples, which, respectively, spiked with *Pseudomonas putida* and *E. coli*. While for virus manipulation, Ness et al. [43] demonstrate extraction and enrichment of MS2 virus from human nasopharyngeal samples by integration of acoustic force to remove host cells, debris, and pollen from the sample and later with electric field force to attract the virus, which is a negatively charged species, and to migrate from sample to co-flowing buffer. Further, Park et al. [44] perform washing and screening of prostate-specific antigen (PSA)-binding aptamer, a single-stranded DNA (ssDNA), using an acoustophoretic separation. The ssDNA pool comprising

of ssDNA library is incubated with microbeads which modified with target molecule, before it is introduced to acoustophoretic separation device, where the microbeads with target-bound DNA fragments are focused on central buffer due to acoustophoretic force, while unbound protein and ssDNA are remained in the original buffer at the side flow. The target-bound DNA on the microbeads is collected and amplified by PCR for subsequent round of washing and screening. Recently, Kennedy et al. [45] communicate the process of purifying target biomolecules utilizing acoustic standing wave in a fluidic chamber to partition and maintain solid-phase bead in an acoustically fluidized bed format, for capturing, washing, and elution of target biomolecules, including monoclonal antibody by protein A beads from a crude cell culture system and recombinant green fluorescent protein (GFP) by anion exchange of a crude cell lysate.

6. Thermophoresis

Thermophoresis (THM) is the motion of particles driven by thermal gradients in the suspending medium. Thermal gradients are commonly generated by local absorption of infrared (IR) laser. The thermal gradients induce diffusional motion of the particles, either toward higher or lower temperature regions [10].

6.1. Fundamentals of THM

Thermophilic particles diffused to the region with higher temperature, while thermophobic particles move to the opposite direction, as shown in **Figure 4a**.

Liquid flow density, J, driven by thermophoretic field, is governed by

$$J = D\left[\nabla C + S_T C(1 - C)\nabla T\right] \tag{10}$$

where D is the diffusion coefficient, C is the concentration, T is the temperature, and S_T is the Soret coefficient, defined as the ratio of thermal diffusion coefficient, D_T, over diffusion coefficient, D, which is given by

$$S_T = \frac{D_T}{D} \tag{11}$$

Steady-state concentration changes for a given spatial temperature difference, ΔT, which is given by

$$\frac{C_{hot}}{C_{cold}} = exp\left(-S_T \Delta T\right) \tag{12}$$

where C_{hot} is the molecule concentration in the hot area, while C_{cold} is in the cold area.

Studies prove that a temperature difference between 2 and 8 K in the beam center with a $1/e^2$ diameter of 25 μm managed to induce thermophoretic motion, while the "$1/e^2$ diameter" (e = 2.71828) indicates the beam diameter where intensity drops to 13.5% of the maximum

value. The temperature rise of the suspending medium must be kept low to avoid bioparticle damage, such as in the case of DNA, which is from 23 to 31°C [47].

6.2. Thermophoretic manipulation of bioparticles

Thermophoretic manipulation of yeast cells has been demonstrated by Lin et al. [46] using low-power and flexible all-optical manipulation method, which presented in **Figure 4b**. They generate light-controlled temperature gradient field thus to trap the suspended cells due to permittivity gradient in the electric double layer of the cell membrane-charged surface. In fact, they manage to realize arbitrary spatial arrangement, as well as precise rotation of single-cell assemblies, with resolution down to 100 nm. J. Chen et al. [48] demonstrate thermophoretic manipulation of *E. coli* by inducing thermal gradient by microscale electric thermal heater. The electric thermal heater is fabricated by gold thin film by means of direct writing with a femtosecond laser. A thin SiO_2 is coated over the gold thin film to electrically isolate the sample as well as to ensure that the trapping is entirely due to thermal effect. Osterman et al. [49] use microscale thermophoresis to study all potential intraviral protein-protein interactions of hepatitis E virus in order to understand the viral replication cycle. The thermal gradient is generated using 100 V-powered red LED for 25 s radiation. Remarkable thermophoretic manipulation of nucleic acids has been demonstrated by He et al. [50], in which translocation of DNA through nanopore utilizing cross-pore thermal gradient has been achieved. Heating of *cis* chamber is performed by exterior heater to maintain the environment at the melting temperature of the double-strand DNA to transform into single-strand DNA. Extensive temperature drop across the pore is caused by thermal-insulating membrane that separate the *cis* and *trans* chambers, resulting in the thermophoretic translocation of the DNA from *cis* to *trans* chamber. Wolff et al. [51] perform microscale thermophoresis upon different forms of the protein α-synuclein, which is associated with Parkinson's disease, to quantitatively characterize

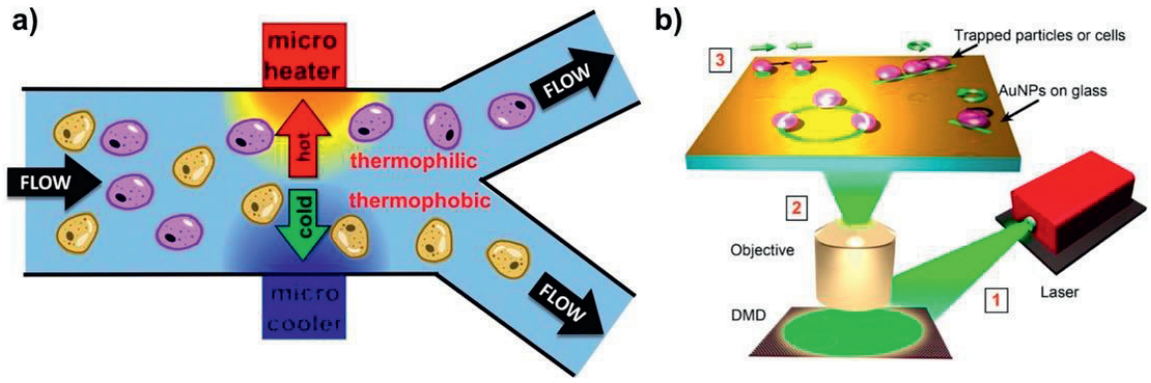

Figure 4. (a) Thermophoresis. Thermophilic bioparticles A (purple) diffuse to regions with higher temperature, while thermophobic bioparticles B (yellow) diffuse to lower temperature regions (Reprinted with permission from Md Ali et al. [13]. Copyright 2016 Royal Society of Chemistry). (b) Manipulation of model organisms by thermophoresis. Optothermal thermophoretic tweezer manipulation is performed by the following: (1) Laser is directed to the digital micromirror device (DMD). (2) Resultant image is focused on gold nanoparticle (AuNP) substrate for surface plasmon excitation. (3) Plasmon-enhanced optothermal potentials defined by the DMD-controlled optical images are exploited to trap and arbitrarily manipulate colloidal particles or biological cells (Adapted with permission from Lin et al. [47]. Copyright 2017 American Chemical Society).

the thermophoretic behavior of the monomeric, oligomeric, and fibrillary forms of the protein. An infrared laser is focused inside a capillary borosilicate where homogenous protein suspension is placed, to generate localized heating, resulting in the motion of the molecules along the temperature gradient until the steady state is established.

7. Optical tweezing/trapping

Optical tweezing or trapping (OPT) indicates the manipulation of particles using optical forces, referring to the exploitation of light radiation pressure to displace and demobilize target particles [11, 12].

7.1. Fundamentals of OPT

Emission of light by a light source induces scattering and gradient forces, which affect particle in the light propagation axis. Scattering force, F_{scat}, affects in the direction of propagation, pushing the particle away from the light source. Gradient force, F_{grad}, on the other hand, affects the direction of the optical field gradient, attracting the particle to the region with peak spatial light intensity [11] as shown in **Figure 5a**.

Optical tweezing or trapping depends on the dimension range of the particle under manipulation, which is governed by two physical principles, i.e., (1) *Mie* scattering and (2) *Rayleigh* scattering [12]. *Mie* regime condition governs for the condition where the particle dimension range is greater than the wavelength of light ($d >> \lambda$) which can be explained by ray optics. Cell-type bioparticle (micron-sized) manipulation lies on this regime. Rays of light carry momentum and

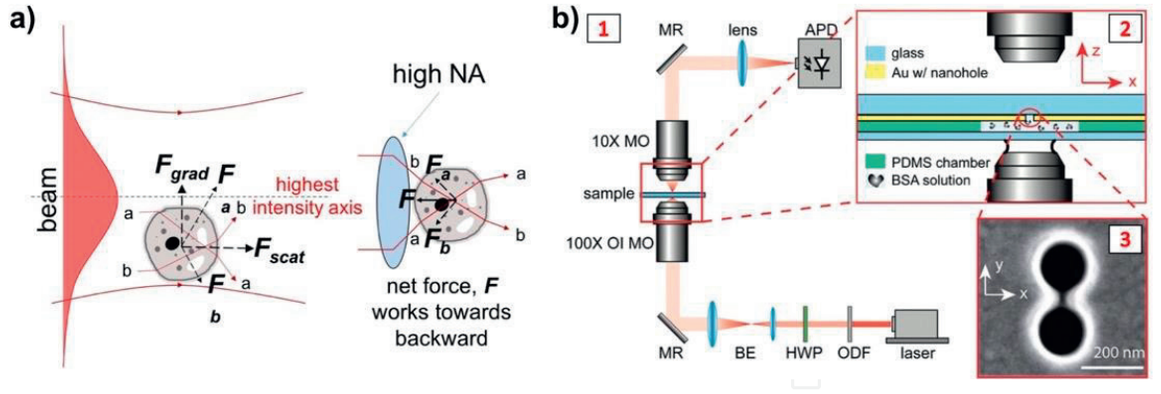

Figure 5. (a) Optical tweezing or trapping. (Left) Scattering force, F_{scat}, pushes bioparticle away from the light source following the direction of light propagation. Gradient force, F_{grad}, attracts bioparticle to the spatial light intensity peak according to the direction of the optical field gradient. (Right) Bioparticle is trapped at the highest intensity region, i.e., light focus, as emission of light through a high numerical aperture number lens generates $F_{grad} > F_{scat}$ condition (Reprinted with permission from Md Ali et al. [13]. Copyright 2016 Royal Society of Chemistry). (b) Manipulation of protein by optical tweezing or trapping: (1) Double-nanohole optical tweezer setup. (2) Details of manipulation of microfluidic device construct. Proteins are trapped at the focus of optical trap at the vicinity of the gold nanohole surface while at the same time unfolding between the double nanoholes. (3) SEM image of the double nanohole (ODF, optical density filter; HWP, half-wave plate; BE, beam expander; MR, mirror; MO, microscope objective; OI MO, oil immersion microscope objective; APD, avalanche photodiode) (Reprinted with permission from Pang and Gordon [52]. Copyright 2011 American Chemical Society).

is refracted when passing through a particle with a refractive index, n_2, which is greater than the surrounding medium, n_1. The rate of the momentum change in the detected rays develops an equal and opposite rate of momentum change of the particle, producing a force by Newton's second law due to conservation of momentum. When a particle is placed in a light gradient, the sum of all rays passing through it creates an imbalance in force, pushing the particle toward the region with higher intensity of light. A focus constructs a trap as the strong light gradient points to the center. *Rayleigh* regime governs for bioparticles with dimension far less than the wavelength ($d \ll \lambda$), such as protein and nucleic acids. In this regime, the particles are treated as extremely small point dipoles polarized by a uniform electric field, which then interacts with light field. The dipole moment, p_{dipole}, induced by a uniform electric field E, is given by

$$p_{dipole} = 4\pi n_{\mathrm{m}}^2 \varepsilon_0 a^3 \left(\frac{m^2-1}{m^2+2}\right) E \tag{13}$$

where n_{1m} and n_{2p} are refractive indices of the suspending medium and the particle, respectively, a is the particle radius, ε_0 is the vacuum permittivity, and m is the contrast ratio of the indices, i.e., $m = n_p/n_m$. The magnitudes of scattering force, F_{scat}, and gradient force, F_{grad}, based on point dipole interaction with light field method are given by

$$F_{scat} = \frac{8\pi n_{\mathrm{m}} k^4 a^6}{3c}\left(\frac{m^2-1}{m^2+2}\right) I \tag{14}$$

$$F_{grad} = \frac{2\pi n_{\mathrm{m}} a^3}{c}\left(\frac{m^2-1}{m^2+2}\right) \nabla I \tag{15}$$

where F_{scat} is the scattering force, F_{grad} is the gradient force, I is the light intensity, c is the speed of light, k is the wave number ($k = 2\pi/\lambda$), and λ is the wavelength. Trapping is achieved at the highest intensity axis when $F_{grad} > F_{scat}$.

OPT can be created by light emission through a high numerical aperture number (NA) of microscope objective (MO), which focuses light tightly and results in a force along the highest intensity axis, but in the backward direction, which causes the bioparticle to be demobilized, as presented in **Figure 5a**.

7.2. Optical tweezing or trapping of bioparticles

Favre-Bulle et al. [53] use optical trapping in vivo to manipulate otoliths in larval zebrafish to stimulate the vestibular system. Lateral and medial forces upon the otolith cause complementary corrective tail motion, while lateral force on either otolith causes a rolling correction in both eyes. Fascinating manipulation of blood has been demonstrated by Zhong et al. [54], who perform manipulation of RBCs in vivo, i.e., within subdermal capillaries in living mice, using infrared optical tweezers. They demonstrate the optical trapping and three-dimensional manipulation of single RBC in the capillary, as well as multiple RBC trapping, forming capillary blockage and clearance, by turning on and off the optical tweezer. Pradhan et al. [55] use optical trapping to bring a single cell of neural tumor cell lines into close proximity of another and measure the time required for cell-cell adhesion to form, as this method can be used to assess the differentiation

status of cancerous cells. They perform the measurement for human neuroblastoma SK-N-SH and rat C6 glioma cells. Stem cell manipulation has been performed by Kirkham et al. [56]. They develop remarkable holographic optical tweezer and demonstrate the micromanipulation of several stem cells, including mouse embryonic stem cells, mouse mesenchymal stem cells, and mouse primary calvarea cells, as well as microstructures, such as poly(DL-lactic-co-glycolic acid) microparticles and electrospun fiber fragments. They succeeded in accurately construct three-dimensional architecture with varying geometries from cocultured cells and microstructure and then stabilized them using hydrogels and cell-cell adhesion methods. Zakrisson et al. [57] perform the optical trapping of nonpiliated strain of *E. coli* bacteria, as well as transformed strain HB101/pHMG93 (expressed as P pili) and the HB101/pAZZ50 strain (expressed as S_{II} pili) in the development of method to determine the presence of pili on a single bacterium. The method comprises of measurement of the bacterium by imaging, then estimation of the fluid drag using an analytical model based on the size, and measurement of the effective fluid drag by oscillating the sample, while the single bacterium is trapped by an optical tweezer. Variation between estimation and measured fluid drag determines the existence of pili. Progress in virus manipulation has been shown by Pang et al. [58]. They conduct optical trapping of individual human immunodeficiency virus (HIV-1) in culture fluid under native conditions and then subsequently perform multiparameter analysis of individual virions, including diameter measurement, concentration-dependent aggregation, and monitoring of viral protein using two-photon fluorescence. Nucleic acid optical manipulation has been achieved by Ngo et al. [59] who use single-molecule assay which integrates fluorescence and optical tweezers generated by infrared laser to manipulate a single nucleosome under force and simultaneously analyze its local conformational transitions. The nucleosome is affixed to a polyethylene glycol (PEG)-coated glass surface at one end of the DNA and pulled via a λ-DNA tethered to the other end by an optical trap to apply force. Pang and Gordon [52], as shown in **Figure 5b**, perform optical trapping and stable unfolding of an individual BSA molecule using a double nanohole in a gold film. The double nanohole with 15 nm separated sharp tips is milled on Au/Ti/glass substrate by a focused ion beam, while the optical trap is generated by 820 nm laser focused onto the sample using a 100× oil immersion microscope objective in a polarization with electric field aligned with the tips of the double nanohole.

8. Conclusion and future perspectives

Manipulation of bioparticles in micro-/nanofluidic, integrated with active manipulation mechanisms, i.e., dielectrophoresis, magnetophoresis, acoustophoresis, thermophoresis, and optical tweezing/trapping, has been discussed in this chapter. Description of the underlying fundamental theory is provided at the beginning, and state-of-the-art implementations into a wide range of bioparticles are carefully introduced. DEP has shown rapid progress into exploration of extremely small bioparticle manipulation, i.e., virus, nucleic acids, and protein. In particular, demonstration of DNA sorting [23] and impedance-based protein capturing [25] prove the potential for nanoscale application, as well as genetic and molecular biology studies. MAG is advantageous in selective manipulation benefited by biofunctionalization of magnetic micro-/nanoparticle for affinity binding to target bioparticles. Novel achievement in customization of

target bioparticle magnetization using predefined multiple layers of magnetic particles [27] is promising for application into heterogeneous suspension manipulation, such as whole blood, progenitor, and cancerous cell detection and sorting. ACT's greatest progress is in the integration with other mechanisms, e.g., DEP, to establish a complete biomedical device [42], showing that transformation from conventional devices to microfluidic biomedical devices which are superfast, precise, and portable is soon to be realized. THM technology particularly is matured enough in extremely small bioparticle manipulation, i.e., protein and nucleic acids, specifically as a measurement tool for binding interaction between molecules. In fact, the recent exploration of thermal gradient-based DNA translocation [50], as well as cell arbitrary manipulation benefited from permittivity gradient in the electric double layer of cell membrane [47], potentially open for new path in THM research. OPT has emerged into in vivo studies [53, 54], indicating that the clinical application is promising and soon to be achieved. In addition, OPT capability in application to genetic and stem cell studies is of high potential, as demonstrated in construction of three-dimensional bioparticle assemblies [55, 56]. Rapid progress of studies on these micro-/nanofluidic active manipulation mechanisms toward bioparticles has a significant impact to biomedical research and technology development. Evolution into high-precision, superfast, and portable miniaturized biomedical devices is pretty soon to be achieved.

Author details

Mohd Anuar Md Ali[1], Aminuddin Bin Ahmad Kayani[2,3]* and Burhanuddin Yeop Majlis[1]

*Address all correspondence to: aminuddin.kayani@mmu.edu.my

1 Institute of Microengineering and Nanoelectronics (IMEN), Universiti Kebangsaan (UKM), Bangi, Selangor, Malaysia

2 Center for Advanced Materials and Green Technology, Multimedia University (MMU), Cyberjaya, Selangor, Malaysia

3 Functional Materials and Microsystems Research Group, School of Engineering, RMIT University, Melbourne, Australia

References

[1] Alberts B, Johnson A, Lewis J, et al. Molecular Biology of the Cell. New York: Garland Science; 2008

[2] Kayani AA, Khoshmanesh K, Ward SA, Mitchell A, Kalantar-zadeh K. Optofluidics incorporating actively controlled micro- and nano-particles. Biomicrofluidics. 2012;**6**:31501

[3] Çetin B, Özer MB, Solmaz ME. Microfluidic bio-particle manipulation for biotechnology. Biochemical Engineering Journal. 2014;**92**:63-82

[4] Sheikholeslami M. Numerical investigation of nanofluid free convection under the influence of electric field in a porous enclosure. Journal of Molecular Liquids. 2018;**249**:1212-1221

[5] Whitesides GM. The origins and the future of microfluidics. Nature. 2006;**442**:368-373

[6] Pohl HA. Dielectrophoresis: The Behavior of Neutral Matter in Nonuniform Electric Fields. Cambridge/New York: Cambridge University Press; 1978

[7] Voldman J. Electrical forces for microscale cell manipulation. Annual Review of Biomedical Engineering. 2006;**8**:425-454

[8] Zborowski M, Chalmers JJ. Magnetophoresis: Fundamentals and applications. In: Webster JG, editor. Wiley Encyclopedia of Electrical and Electronics Engineering. Chichester: Wiley; 2015. pp. 1-23

[9] Lenshof A, Laurell T. Acoustophoresis. In: Bhushan B, editor. Encyclopedia of Nanotechnology. Springer: Dordrecht; 2012. pp. 45-50

[10] Reineck P, Wienken CJ, Braun D. Thermophoresis of single stranded DNA. Electrophoresis. 2010;**31**:279-286

[11] Ashkin A. Acceleration and trapping of particles by radiation pressure. Physical Review Letters. 1970;**24**:156-159

[12] Woerdemann M. Structured Light Fields: Applications in Optical Trapping, Manipulation, and Organisation. Berlin/Heidelberg: Springer; 2012

[13] Md Ali MA, Ostrikov K (Ken), Khalid FA, Majlis BY, Kayani AA. Active bioparticle manipulation in microfluidic systems. RSC Advances. 2016;**6**:113066-113094

[14] D'Amico L, Ajami NJ, Adachi JA, Gascoyne PRC, Petrosino JF. Isolation and concentration of bacteria from blood using microfluidic membraneless dialysis and dielectrophoresis. Lab on a Chip. 2017;**17**:1340-1348

[15] Çetin B, Li D. Dielectrophoresis in microfluidics technology. Electrophoresis. 2011;**32**: 2410-2427

[16] Jones TB. Basic theory of dielectrophoresis and electrorotation. IEEE Engineering in Medicine and Biology Magazine. 2003;**22**:33-42

[17] Muratore M, Mitchell S, Waterfall M. Plasma membrane characterization, by scanning electron microscopy, of multipotent myoblasts-derived populations sorted using dielectrophoresis. Biochemical and Biophysical Research Communications. 2013;**438**:666-672

[18] Chen X, Liang Z, Li D, et al. Microfluidic dielectrophoresis device for trapping, counting and detecting Shewanella oneidensis at the cell level. Biosensors & Bioelectronics. 2018;**99**:416-423

[19] Sang S, Feng Q, Jian A, et al. Portable microsystem integrates multifunctional dielectrophoresis manipulations and a surface stress biosensor to detect red blood cells for hemolytic anemia. Scientific Reports. 2016;**6**:33626

[20] Chiu T-K, Chou W-P, Huang S-B, et al. Application of optically-induced-dielectrophoresis in microfluidic system for purification of circulating tumour cells for gene expression analysis- Cancer cell line model. Scientific Reports. 2016;**6**:32851

[21] Adams TNG, Jiang AYL, Vyas PD, Flanagan LA. Separation of neural stem cells by whole cell membrane capacitance using dielectrophoresis. Methods. 2018;**133**:91-103

[22] Ding J, Lawrence RM, Jones PV, Hogue BG, Hayes MA. Concentration of Sindbis virus with optimized gradient insulator-based dielectrophoresis. Analyst. 2016;**141**:1997-2008

[23] Jones PV, Salmon GL, Ros A. Continuous separation of DNA molecules by size using insulator-based Dielectrophoresis. Analytical Chemistry. 2017;**89**:1531-1539

[24] Viefhues M, Regtmeier J, Anselmetti D. Nanofluidic devices for dielectrophoretic mobility shift assays by soft lithography. Journal Micromechanics Microengineering. 2012;**22**:115024

[25] Mohamad AS, Hamzah R, Hoettges KF, Hughes MP. A dielectrophoresis-impedance method for protein detection and analysis. AIP Advances. 2017;**7**:15202

[26] Liao K, Chaurey V, Tsegaye M, Chou C, Swami NS. Nanofluidics for selective protein trapping in bio-fluids. In: Landers JP, editor. Fifteenth International Conference on Miniaturized Systems for Chemistry and Life Sciences. San Diego: Chemical and Biological Microsystems Society; 2011. pp. 1071-1073

[27] Lee H, Hong D, Cho H, et al. Turning diamagnetic microbes into multinary micromagnets: Magnetophoresis and spatio-temporal manipulation of individual living cells. Scientific Reports. 2016;**6**:38517

[28] Schneider T, Moore LR, Jing Y, et al. Continuous flow magnetic cell fractionation based on antigen expression level. Journal of Biochemical and Biophysical Methods. 2006;**68**:1-21

[29] Zeng J, Deng Y, Vedantam P, Tzeng T-R, Xuan X. Magnetic separation of particles and cells in ferrofluid flow through a straight microchannel using two offset magnets. Journal of Magnetism and Magnetic Materials. 2013;**346**:118-123

[30] Jin X, Abbot S, Zhang X, et al. Erythrocyte enrichment in hematopoietic progenitor cell cultures based on magnetic susceptibility of the hemoglobin. PLoS One. 2012;**7**:e39491

[31] Jack R, Hussain K, Rodrigues D, et al. Microfluidic continuum sorting of sub-populations of tumor cells via surface antibody expression levels. Lab on a Chip. 2017;**17**:1349-1358

[32] Wang ZM, Wu RG, Wang ZP, Ramanujan RV. Magnetic trapping of Bacteria at low magnetic fields. Scientific Reports. 2016;**6**:26945

[33] Wang Y, Li Y, Wang R, Wang M, Lin J. Three-dimensional printed magnetophoretic system for the continuous flow separation of avian influenza H5N1 viruses. Journal of Separation Science. 2017;**40**:1540-1547

[34] Shim S, Shim J, Taylor WR, et al. Magnetophoretic-based microfluidic device for DNA concentration. Biomedical Microdevices. 2016;**18**:28

[35] Lim B, Torati SR, Kim KW, Hu X, Reddy V, Kim C. Concentric manipulation and monitoring of protein-loaded superparamagnetic cargo using magnetophoretic spider web. NPG Asia Materials. 2017;**9**:e369

[36] Antfolk M, Antfolk C, Lilja H, Laurell T, Augustsson P. A single inlet two-stage acoustophoresis chip enabling tumor cell enrichment from white blood cells. Lab on a Chip. 2015;**15**:2102-2109

[37] Destgeer G, Alazzam A, Sung HJ. High frequency travelling surface acoustic waves for microparticle separation. Journal of Mechanical Science and Technology. 2016;**30**:3945-3952

[38] Ohlsson P, Evander M, Petersson K, et al. Integrated acoustic separation, enrichment, and microchip polymerase chain reaction detection of bacteria from blood for rapid sepsis diagnostics. Analytical Chemistry. 2016;**88**:9403-9411

[39] Sundvik M, Nieminen HJ, Salmi A, Panula P, Hæggström E. Effects of acoustic levitation on the development of zebrafish, Danio rerio, embryos. Scientific Reports. 2015;**5**:13596

[40] Urbansky A, Lenshof A, Dykes J, Laurell T, Scheding S. Affinity-bead-mediated enrichment of CD8+ lymphocytes from peripheral blood progenitor cell products using acoustophoresis. Micromachines. 2016;**7**:101

[41] Urbansky A, Ohlsson P, Lenshof A, Garofalo F, Scheding S, Laurell T. Rapid and effective enrichment of mononuclear cells from blood using acoustophoresis. Scientific Reports. 2017;**7**:17161

[42] Antfolk M, Kim SH, Koizumi S, Fujii T, Laurell T. Label-free single-cell separation and imaging of cancer cells using an integrated microfluidic system. Scientific Reports. 2017;**7**:46507

[43] Ness K, Rose KA, Jung B, Fisher K, Mariella RP Jr. Improved bacterial and viral recoveries from complex samples using electrophoretically assisted acoustic focusing. In: Locascio LE, editor. Twelfth International Conference on Miniaturized Systems for Chemistry and Life Sciences. San Diego: Chemical and Biological Microsystems Society; 2008. pp. 802-804

[44] Park JW, Lee SJ, Ren S, Lee S, Kim S, Laurell T. Acousto-microfluidics for screening of ssDNA aptamer. Scientific Reports. 2016;**6**:27121

[45] Kennedy T, Pluskal M, Gilmanshin R, Lipkens B. Acoustophoresis mediated chromatography processing: Capture of proteins from cell cultures. The Journal of the Acoustical Society of America. 2017;**141**:3505

[46] Yu L-H, Chen Y-F. Concentration-dependent thermophoretic accumulation for the detection of DNA using DNA-functionalized nanoparticles. Analytical Chemistry. 2015;**87**:2845-2851

[47] Lin L, Peng X, Wei X, Mao Z, Xie C, Zheng Y. Thermophoretic tweezers for low-power and versatile manipulation of biological cells. ACS Nano. 2017;**11**:3147-3154

[48] Chen J, Cong H, Loo FC, et al. Thermal gradient induced tweezers for the manipulation of particles and cells. Scientific Reports. 2016;**6**:35814

[49] Osterman A, Stellberger T, Gebhardt A, et al. The hepatitis E virus intraviral interactome. Scientific Reports. 2015;**5**:13872

[50] He Y, Tsutsui M, Scheicher RH, Bai F, Taniguchi M, Kawai T. Thermophoretic manipulation of DNA translocation through nanopores. ACS Nano. 2013;**7**:538-546

[51] Wolff M, Mittag JJ, Herling TW, et al. Quantitative thermophoretic study of disease-related protein aggregates. Scientific Reports. 2016;**6**:22829

[52] Pang Y, Gordon R. Optical trapping of a single protein. Nano Letters. 2012;**12**:402-406

[53] Favre-Bulle IA, Stilgoe AB, Rubinsztein-Dunlop H, Scott EK. Optical trapping of otoliths drives vestibular behaviours in larval zebrafish. Nature Communications. 2017;**8**:630

[54] Zhong M-C, Wei X-B, Zhou J-H, Wang Z-Q, Li Y-M. Trapping red blood cells in living animals using optical tweezers. Nature Communications. 2013;**4**:1768

[55] Pradhan M, Pathak S, Mathur D, Ladiwala U. Optically trapping tumor cells to assess differentiation and prognosis of cancers. Biomedical Optics Express. 2016;**7**:943-948

[56] Kirkham GR, Britchford E, Upton T, et al. Precision assembly of complex cellular micro-environments using holographic optical tweezers. Scientific Reports. 2015;**5**:8577

[57] Zakrisson J, Singh B, Svenmarker P, et al. Detecting bacterial surface organelles on single cells using optical tweezers. Langmuir. 2016;**32**:4521-4529

[58] Pang Y, Song H, Kim JH, Hou X, Cheng W. Optical trapping of individual human immunodeficiency viruses in culture fluid reveals heterogeneity with single-molecule resolution. Nature Nanotechnology. 2014;**9**:624-630

[59] Ngo TTM, Zhang Q, Zhou R, Yodh JG, Ha T. Asymmetric unwrapping of nucleosomes under tension directed by DNA local flexibility article asymmetric unwrapping of nucleosomes under tension directed by DNA local flexibility. Cell. 2015;**160**:1135-1144